JCI The Journal of Clinical Investigation

Melanocortin 4 receptor stimulation prevents anti-depressant-associated weight gain in mice caused by long-term fluoxetine exposure

Maria Jose Ortuno, … , Jeffrey M. Friedman, Patricia Ducy

J Clin Invest. 2021. https://doi.org/10.1172/JCI151976.

Research In-Press Preview **Metabolism**

Graphical abstract

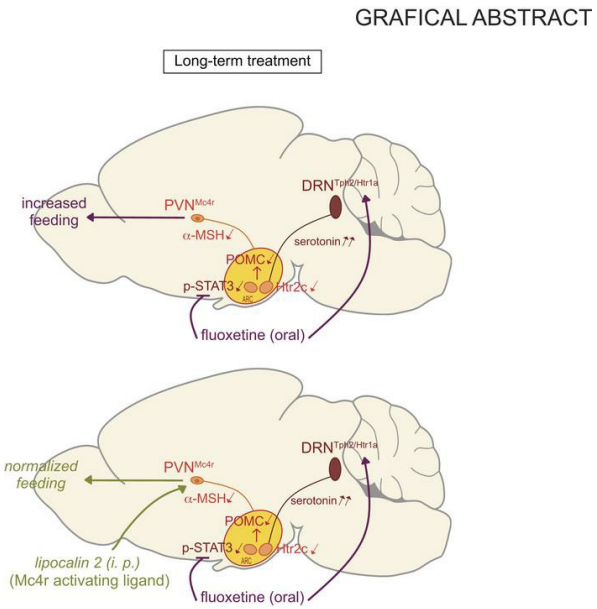

Melanocortin 4 receptor stimulation prevents anti-depressant-associated weight gain in mice caused by long-term fluoxetine exposure

María José Ortuño[1*], Marc Schneeberger[2], Anoj Ilanges[2], François Marchildon[3], Kyle Pellegrino[2], Jeffrey M. Friedman[2], Patricia Ducy[4,5*]

[1]Department of Genetics and Development, College of Physicians and Surgeons, Columbia University, New York, NY 10033, USA.

[2]Laboratory of Molecular Genetics, Howard Hughes Medical Institute, The Rockefeller University, New York, NY 10065, USA.

[3]Laboratory of Molecular Metabolism, The Rockefeller University, New York, NY, 10065, USA.

[4]Department of Pathology and Cell Biology, College of Physicians and Surgeons, Columbia University, New York, NY 10033, USA.

[5]Lead contact.

*Correspondence to: Patricia Ducy and Maria Jose Ortuno. Columbia University Medical Center. Black Building, room BB1412, 650 W 168th Street, New York, NY 10033, USA. Phone: (212) 305-9299; E-mails: pd2193@cumc.columbia.edu and mjo2129@cumc.columbia.edu.

The authors have declared that no conflict of interest exists.

Abstract: Contrasting with the predicted anorexigenic effect of increasing brain serotonin signaling, long-term use of selective serotonin reuptake inhibitors (SSRIs) antidepressants correlates with body weight gain. This adverse outcome increases the risk of transitioning to obesity and interferes with treatment compliance. Here we show that orally administered fluoxetine (Flx), a widely prescribed SSRI, increased body weight by enhancing food intake in healthy mice at two different time points and through two distinct mechanisms. Within hours, Flx decreased the activity of a subset of brainstem serotonergic neurons by triggering autoinhibitory signaling through the Htr1a receptor. Upon longer treatment Flx blunted Htr2c expression/signaling, decreased the phosphorylation of Creb and Stat3 and dampened the production of POMC/α-MSH in hypothalamic neurons, thereby increasing food intake. Accordingly, exogenous stimulation of the melanocortin 4 receptor (MC4R) by co-treating mice with Flx and lipocalin-2, an anorexigenic hormone signaling through this receptor, normalized feeding and body weight. Flx and other SSRIs also inhibit CREB/STAT3 phosphorylation in a human neuronal cell line suggesting that these non-canonical effects could also occur in long-term users of SSRIs. By defining the molecular basis of the long-term SSRIs-associated weight gain this study proposes a therapeutic strategy to counter it.

INTRODUCTION

Selective serotonin reuptake inhibitors (SSRIs) are the most widely prescribed antidepressants in western countries. Chief among them is fluoxetine, the active compound in Prozac, whose number of prescription in the US reached over 25 millions in 2018 (1). SSRIs increase serotonin in the synaptic cleft by preventing reuptake by the sertonin transporter (SERT) in pre-synaptic neurons, leading to enhanced signaling in post-synaptic neurons (2, 3). Given the well-described anorectic effect of brain serotonin signaling (4, 5), SSRIs would be predicted to decrease food intake. Indeed, early studies have shown that rats injected with fluoxetine lose weight (6, 7). Moreover, in the first months of treatment some SSRIs users lose weight, a manifestation consistent with the predicted tempering effect of enhanced central serotonin signaling on the regulation of feeding (8, 9). However, a growing number of clinical studies are reporting that the long-term

use (≥ 1 year) of SSRIs is instead associated with weight gain (10-15). This paradoxical weight gain, which ranks as the third most common side effect of these drugs by users (16), has become a major concern for clinicians since it not only increases the long-term risk of metabolic syndrome but is also one of the most common reasons for premature discontinuation of the treatment (12, 13, 15). Given that SSRIs are increasingly prescribed and that more than a third of patients uses them for longer than 2 years, this concern keeps mounting (16, 17) (https://www.cdc.gov/nchs/products/databriefs/db283.htm). There is therefore a strong interest in understanding the biological basis of this paradoxical side effect to define therapeutic strategies to counter it.

RESULTS

Both a short-term and a long-term treatment with oral fluoxetine increase food intake.

To investigate the mechanism causing weight gain following long-term treatment with SSRIs we analyzed the effect of fluoxetine (Flx), one of the most prescribed SSRIs worldwide. We mimicked SSRI administration in humans by providing Flx orally to wild-type (WT) healthy mice at a dose that results in plasma concentrations comparable to therapeutic levels achieved in humans (18) (Supplemental Figure 1A). In these conditions, mice significantly gained weight and adiposity compared to vehicle-treated controls following a 6 week-long treatment (Figure 1, A and B, and Supplemental Figure 1, B to D and F). Lengthening the treatment to 12 weeks in another group of mice did not modify these parameters (Figure 1, A and B and Supplemental Figure 1, E and F). To define which variables in the energy balance equation were responsible for this weight gain, we assessed the influxes (feeding) and outfluxes (energy expenditure) of energy in mice treated with Flx for 6-weeks. None of the parameters associated with energy expenditure i.e., basal metabolic rate, thermogenesis and physical activity was changed by the Flx treatment (Figure 1, C and D). In contrast, daily averaged and cumulative food intake over the last 5 days were significantly higher in Flx- compared to vehicle-treated mice (Figure 1E and Supplemental Figure 1G). When reported to body weight, cumulative food intake was also significantly increased by the Flx treatment while daily food

intake trended upward but did not reach significance (Supplemental Figure 1, H and I). These results support the notion that, in mice, the increased body weight caused by a long-term oral treatment with Flx is maintained by increased food intake.

In the course of our analysis, we noticed that body weight, fat mass and cumulative food intake were already increased after 5 days of treatment with oral Flx in mice of both sexes (Figure 2, A to C and Supplemental Figure 2, A to G). A day-by-day analysis revealed that Flx increases feeding daily and as early as within the first 24h (Figure 2D and Supplemental Figure 2H). More specifically, a 14h treatment during the active (dark) phase of the day was sufficient to trigger a significant increase in food intake compared to vehicle-treated controls (Figure 2E and Supplemental Figure 2I). As with the long-term treatment, averaged metabolism, thermogenesis and physical activity were not changed by this acute Flx treatment in males and females (Figure 2, F and G and Supplemental Figure J to M). A day-by-day analysis in females did not either reveal any difference prior to body weight/adiposity divergence between vehicle- and Flx-treated groups (Supplemental Figure 2, N and O). Thus, when given orally to mice, Flx causes weight gain by increasing food intake in an acute manner as well as in a long-term mode.

The short-term orexigenic effect of fluoxetine is mediated by an autoinhibitory effect in serotonergic neurons of the dorsal raphe nuclei.

To identify central sites which activity is acutely altered by Flx in an unbiased manner, we compared averaged maps of c-Fos-positive (Fos^+) i.e., recently activated, neurons in intact whole brains of vehicle- and Flx-treated female mice using the tissue clearing/immunolabelling technique iDISCO+ paired to the cell detection and registration software ClearMap. A 3D automated comparison between p-value maps of c-Fos expression and the Allen Brain Atlas annotation (© 2015 Allen Institute for Brain Science, brain-map.org/api/index.html) identified 3 known regulatory centers of feeding, the dorsal raphe nucleus (DRN) of the brainstem, the arcuate nucleus (ARC) and the paraventricular nucleus (PVN) of the hypothalamus as low Fos^+ areas in Flx- compared to vehicle-treated mice (Figure 3, A and B and Supplemental Figure 3, A

and B). These results were validated in coronal brain slices using conventional immunohistofluorescence (IHF) (Figure 3C). Next, to specify which subsets of neurons within these areas are affected by Flx, we assessed the co-localization between c-Fos and known neuronal markers associated with the regulation of feeding. In the DRN, IHF identified a significantly lower number of $Fos^+/Tph2^+$ neurons, a subset of neurons that negatively regulates feeding (19), in Flx- compared to vehicle-treated females (Figure 3D and Supplemental Figure 3C), suggesting that Flx rapidly inhibits these serotonergic neurons. In pro-opiomelanocortin (POMC) neurons of the ARC, which drive satiety (20, 21), POMC levels and the number of $Fos^+/POMC^+$ neurons were decreased after Flx treatment compared to vehicle (Figure 3E and Supplemental Figure 3E), suggesting that Flx also rapidly inhibits these neurons. Accordingly, levels of alpha-melanocyte stimulating hormone (α-MSH), the POMC cleavage product that induces satiety by signaling in PVN (22), were also decreased in Flx- compared to vehicle-treated mice. This decrease manifested as early as 2h after Flx treatment but reached significance after 14h, reflecting the multi-step posttranslational cleavage of POMC required for α-MSH to be secreted (Figure 3F and Supplemental Figure 3, D and F). In contrast, levels of NPY, another regulator of food intake (21), were not affected by the treatment with Flx (Supplemental Figure 3G). To further confirm that Flx affects α-MSH production, a group of mice was treated with Flx for 2h, the drug was then removed and α-MSH levels in the PVN were analyzed by IHF 1 or 2 days later. As shown in Figure 3F, a 2-days withdrawal period normalized the density of α-MSH signal. Altogether, these results identify the serotonin producing neurons in the DRN and the melanocortin circuitry of the hypothalamus as targets and putative mediators of Flx effect on feeding.

POMC neurons neither express *Sert*, the gene encoding the canonical target of Flx, nor do they secrete serotonin ((19, 23) and the Allen Brain Atlas annotation © 2015 Allen Institute for Brain Science, brain-map.org/api/index.html). We therefore examined whether the short-term orexigenic effect of Flx results from a serotonin-dependent cascade originating in the DRN that modulates the melanocortin system in the hypothalamus. We first assessed the effect of oral Flx on neuronal and feeding endpoints in mice lacking brain serotonin due to replacement of *Tph2*, a gene encoding a rate-limiting enzyme in the central serotonin

synthesis cascade, with the *lacZ* reporter gene (ß-Gal)(19). No change in the number of Fos^+/ß-Gal^+ neurons was observed in the DRN of Flx- compared to vehicle-treated *Tph2*-deficient mice whereas the number of Fos^+/$Tph2^+$ neurons in this area was decreased by the Flx treatment in their control WT littermates (Figure 4A and Supplemental Figure 4, A and B). Moreover, *Tph2*-deficient mice treated with Flx exhibited no alteration in the number of Fos^+/$POMC^+$ neurons in the ARC and no decreased levels of α-MSH in the PVN while these effects could be observed in their control WT littermates (Figure 4, B and C and Supplemental Figure 4, C to E). These data suggest that brain serotonin could be required for the short-term effect of Flx on the DRN and POMC neurons of the hypothalamus. Supporting the notion that the acute effect of oral Flx on feeding could be brain serotonin-dependent, no change in food intake or adiposity was observed in *Tph2*-deficient mice after 5 days of Flx treatment while both parameters were increased in Flx-treated WT control littermates (Figure 4, D and E and Supplemental Figure 4, F to I).

The therapeutic effect of Flx relies on an inhibition of serotonin reuptake by SERT that increases serotonin levels in the synaptic cleft (2). Thus, to test whether Flx acts on DRN neurons through this canonical action on SERT, we next analyzed mice lacking its encoding gene (*Slc6a4*) (24). Similar to what was observed in *Tph2*-deficient mice, we found that the number of Fos^+/$Tph2^+$ activated serotonergic neurons in the DRN was unchanged by the Flx treatment in SERT-deficient mice (Figure 4F and Supplemental Figure 4J). Taken together, these results indicate that an acute oral treatment with Flx increases feeding through a direct action on DRN serotonergic neurons and suggest that the changes in hypothalamic POMC and α-MSH levels occurring in the hypothalamus are downstream of this effect.

DRN neurons send ascending projections to the ARC and the PVN, and serotonin signaling through the Htr2c receptor in ARC^{POMC} neurons inhibits food intake (5, 9, 25, 26), an effect opposite to the rapid increase in feeding triggered by the Flx treatment (Figure 2, C and D). DRN neurons express the inhibitory Htr1a serotonin autoreceptor, and Htr1a negative regulation on the production of serotonin has been implicated in the delayed therapeutic efficacy of SSRIs on mood disorders (27, 28). We hypothesized that, by enhancing serotonin availability through SERT blockade, Flx could promote Htr1a negative feedback,

thereby decreasing serotonin production, and signaling in downstream neurons controlling feeding (29). If this hypothesis is correct, blocking Htr1a function should prevent short-term Flx-induced hyperphagia as efficiently as enhancing the activity of Htr2c downstream of this effect. Indeed, co-administration of Flx and propranolol (Prop), which inhibits Htr1a signaling (30), or Flx and lorcaserin (Lorca), a potent Htr2c agonist known to inhibit food intake (9, 31), are both sufficient to prevent increases in feeding, body weight and adiposity induced by Flx (Figure 4, G to N and Supplemental Figure 4, K to N). These observations support the notion that a short-term oral Flx treatment increases food intake through a serotonin-mediated autoinhibition of the $DRN^{Tph2/Htr1a}$ neurons that lowers serotonin production and therefore its signaling in ARC^{POMC} neurons to cause a decrease of α-MSH production.

Impairment of Htr2c expression, loss of Stat3 phosphorylation in ARC neurons and low α-MSH production explain the long-term orexigenic effect of fluoxetine.

To determine whether a similar mechanism causes the long-term orexigenic effect of Flx, mice were treated for 6 weeks with Flx or vehicle, and levels of α-MSH were analyzed by IHF. As seen with the 5 days treatment, long-term exposure to Flx markedly decreased α-MSH levels in the PVN and withdrawal of the drug normalized α-MSH levels after 4 weeks (Figure 5A). These data indicate that the effect of long-term Flx treatment on α-MSH production is reversible. On the other hand, and in contrast to its preventative action on the acute effect of oral Flx on food intake, lorcaserin did not normalize feeding in mice pre-treated for 5 weeks with Flx (Figure 5, B and C). Consequently, the long-term Flx/Lorca co-treated mice gained weight and had an increase in fat mass comparable to controls treated with Flx only (Figure 5, D to F and Supplemental Figure 5, A and B). The difference of lorcaserin impact on the short-term and long-term orexigenic activity of Flx suggests that Htr2c signaling might be impaired and/or that a negative effect on another regulator of α-MSH production is occurring.

We have previously demonstrated that a long-term treatment with Flx decreases Htr2c levels and its activation/phosphorylation of Creb, its downstream effector in the hypothalamic neurons regulating bone

remodeling (32, 33). Since this receptor also mediates serotonin's effect on feeding (34-36), we assessed whether the long-term effect of Flx is associated with a decrease in Htr2c levels in ARC neurons. Double IHF staining confirmed a weakened Htr2c signal in $POMC^+$ ARC neurons in mice treated for 6 weeks with Flx compared to vehicle (Figure 5G, arrows). POMC levels were also decreased in the ARC region (Figure 5H). Given that *POMC* is also expressed in Htr2c-negative neurons of the ARC (36) and that phosphorylated Stat3 (p-STAT3) is a major regulator of its expression (37) we next tested whether Flx affects this transcription factor. We found that p-STAT3 levels were decreased in ARC neurons of mice treated for 6 weeks with Flx (Figure 5I). Hence, upon long-term use Flx decreases α-MSH production by interfering with two pathways regulating *POMC* expression: in one subset of neurons it lowers Htr2c expression and impairs the Creb-dependent activation of the *POMC* promoter (32), and in other neurons it decreases its Stat3-dependent induction by hampering this factor phosphorylation.

Fluoxetine impairs STAT3 phosphorylation, CREB activation and POMC expression in human neuronal cells

To begin evaluating the potential relevance of this dual inhibitory mechanism to human biology, we analyzed the effect of Flx on the human neuroblastoma cell line SH-SY5Y that upon treatment with all-trans-retinoic acid expresses mature neuronal markers (Supplemental Figure 6A). Even though *POMC* expression is low in these cells, it was decreased by a 2h treatment with Flx (Figure 6A), Likewise, western blot analysis respectively identified a 20% and 15% decrease in the p-STAT3/STAT3 ratio and the p-CREB/CREB ratio in Flx-treated cells (Figure 6, B and C). This effect was observed in all experiments and was specific to the p-STAT Tyr-705 form, which is the main form regulating *POMC* expression, as STAT3 ERK-dependent Ser-727 phosphorylation was not affected (Supplemental Figure 6B).

Newer generation SSRIs are also associated with weight gain following long-term use (14). We therefore tested whether several of these compounds were inhibiting STAT3 and/or CREB phosphorylation. As shown in Figure 6D, all four compounds tested decreased CREB phosphorylation in differentiated SY5Y cells although the effect with fluvoxamine did not reach statistical significance. Sertraline, escitalopram, and

fluvoxamine also inhibited STAT3 phosphorylation to the same extent as Flx (Figure 6E). Of note, paroxetine, which does not elicit a significant weight gain in patients (14), did not have a negative effect on this process (Figure 6E).

Pharmacologically enhancing Mc4R activity compensates both Flx short- and long-term anorexigenic effects and blocks weight gain

The results presented above indicate that a decrease in α-MSH signaling in the PVN is ultimately responsible for the paradoxical orexigenic effect of oral Flx. Since α-MSH suppresses hunger by signaling through the melanocortin 4 receptor (Mc4r) expressed on PVN neurons (22), we reasoned that exogenously stimulating Mc4r signaling could block this orexigenic effect. Such treatment should be able to compensate for the decreased α-MSH production caused by both the short-term firing inhibition of DRN^{Tph2} neurons by Htr1a negative feedback and the decrease of hypothalamic Htr2c signaling and Creb/Stat3 activity associated with a long-term Flx treatment. To test this hypothesis, we injected mice with lipocalin-2 (Lcn2), a recently described anorexigenic hormone signaling directly through Mc4r in the hypothalamus (38), either during a 5-days co-treatment or for 5 days after a 5-weeks pre-treatment with Flx (Figure 7A). We observed that, in both cases, the Lcn2 treatment decreased food intake compared to mice treated with Flx alone (Figure 7, B and F). Accordingly, body weight and adiposity were also normalized in mice co-treated with Flx and Lcn2 compared to Flx-treated ones (Figure 7, C to E and G to I, and Supplemental Figure 7, A to E). Importantly, this treatment with Lcn2 did not interfere with the beneficial effect of Flx on mouse behavior, as assayed by the classic marble-burying test measuring anxiety (Figure 7J). Thus, increasing Mc4r signaling in the hypothalamus by peripherally injecting Lcn2 can compensate for the decrease in α-MSH signaling induced by Flx and thereby block its short-term as well as long-term orexigenic effect without affecting its therapeutic benefit.

DISCUSSION

We show here that a long-term oral treatment with fluoxetine promotes weight gain in healthy mice by increasing food intake. This effect is centrally mediated and impinges on the positive regulation of the melanocortin pathway by brain serotonin through two different mechanisms (Figure 8). Flx initially triggers an Htr1a autoinhibition of DRN^{Tph2} neurons of the brainstem that decreases their positive action on ARC^{POMC} neurons. Pharmacologically blocking Htr1a or compensating for the decrease of serotonin signaling by directly stimulating Htr2c with lorcaserin can block this initial orexigenic effect of Flx. When the Flx treatment period is extended, a decrease in hypothalamic Htr2c levels/signaling combined with a negative effect of Flx in ARC neurons on the phosphorylation of Creb and Stat3, two major regulators of *POMC* expression, induces a decrease in α-MSH levels, an increase in food intake and weight gain. In this second phase, lorcaserin has no effect whereas acting downstream of Htr2c/POMC neurons by stimulating Mc4r signaling with lipocalin-2 can block Flx orexigenic effect and hinder weight gain. Our data also show that Flx and other SSRIs can inhibit STAT3 and CREB phosphorylation, and thereby *POMC* expression, in human neuronal cells. Although preliminary, this observation suggests that a similar mechanism could affect feeding in mice and humans and therefore that MC4R agonists could be used to control SSRIs-induced weight gain in patients.

Our observations explain how Flx impinges on known components of the serotonin-melanocortin pathway to reverse its effect on feeding. For instance, the initial Htr1a-mediated inhibition of DRN^{Tph2} neurons activity and its lowering effect on downstream serotonin signaling has been previously described, although in the context of mood and anxiety, not of food intake (27). This negative feedback inhibition in response to increased inter-synaptic serotonin levels in the DRN is believed to account for the delayed therapeutic response to SSRIs; these drugs would be able to achieve their functional effect only once desensitization of Htr1a has occurred (27). Such latter mechanism, however, does not explain the weight loss observed within 24h of treatment in studies performed in rats (6, 7). A major difference between these and our studies relates to the route of Flx administration. We opted for an oral treatment that would more precisely mimic the conditions of administration in patients, whereas these early studies delivered Flx via intraperitoneal

injections. Whether the divergence of effect relates to differences in processing, bioavailability or kinetics of brain concentration remains to be determined. Notably, our results are consistent with previous observations reported in studies delivering Flx orally, although those used different doses and were not designed to evaluate this drug's activity on feeding (39, 40).

While consistent with the body weight gain reported by long-term users of SSRIs, the orexigenic effect of Flx we observe after 6 weeks of treatment conflicts with the effect expected from a drug acting by increasing brain serotonin signaling. This apparent contradiction is explained by the combination of multiple molecular events taking place downstream of serotonin signaling in ARC neurons that our and previous studies uncovered. Indeed, the fact that increased inter-synaptic serotonin levels should trigger Htr2c desensitization (41) combined with the observation that Flx decreases its levels in hypothalamic neurons ((32) and Figure 5G) should dampen serotonin signaling and therefore blunt the potential effect of its SSRIs-mediated increase. The inhibition on the phosphorylation of Stat3 and Creb would add to this loss of Htr2c signaling and concur to prompt the decrease in α-MSH levels we observe. The fact that the Htr2c agonist lorcaserin can block Flx-induced serotonin-dependent initial hyperphagia/weight gain but is ineffective in doing so upon a long-term pre-treatment is consistent with this multilevel block in Htr2c-mediated regulation of feeding.

Our in vitro experiments using differentiated SY5Y-derived neuronal cells suggest that Flx can inhibit *POMC* expression through its negative effect on p-STAT3 and p-CREB in human cells as it does in mouse neurons. While these data cannot be interpreted as modeling the situation in humans, if they could be verified in Flx-treated patients, it would mean that lorcaserin or other compounds enhancing serotonin production or Htr2c signaling may not be successful in blocking such effect in long-term users of SSRIs. Targeting instead the pathway downstream of these factors may a better therapeutic strategy. Specifically, directly stimulating MC4R by injecting the satiety hormone, LIPOCALIN-2 (38), which anorexigenic effect is conserved between rodents, non-human primates and humans (42), could block the effect of Flx on feeding and therefore limit

weight gain in patients. Additional studies analyzing LCN2 pharmacology and safety profile are, however, needed to establish its value as a co-drug and in particular to assess its effect on blood pressure and heart rate, as other MC4R agonists have been clinically abandoned due to unacceptable increases in these parameters (43). In that respect, co-treatment with SSRIs and the MC4R selective agonist setmelanotide may represent a closer option since this drug did not show adverse cardiovascular effects while significantly reducing weight loss and hunger scores in phase III clinical trials in individuals with POMC or LEPR deficiency (44, 45).

METHODS

Study design

The study was performed using mouse models and a human neuron-like cell line. *In vivo*, group sizes were determined by performing a power calculation to lead to an 80% chance of detecting a significant difference ($p \leq 0.05$). All were laboratory-controlled experiments and were designed with specific final endpoints, which were arbitrarily designed to represent acute, short-term and long-term treatments. In all experiments, animals were randomly assigned to the specific treated groups. Any mouse displaying immobility, huddled posture, inability to eat or drink, ruffled fur, self-mutilation, vocalization, wound dehiscence or signs of hypothermia was excluded from the study.

All values use biological replicates and are indicated by group size (*n*) in figure legends or with dots in bar graphs. For *in vivo* data, each "*n"* corresponds to a single mouse. For *in vitro* data, each "*n"* corresponds to a replicate; 2-6 independent experiments were performed with triplicates per condition. Body weight measurements and feeding experiments for WT mice were performed several times, except for the 12-weeks treatment.

Animals and *in vivo* treatments

WT and *Sert*$^{-/-}$ mice were purchased from Jackson Laboratory (Bar Harbor, Maryland). Generation of *Tph2*$^{-/-}$ mice was reported previously (19). All mice were analyzed on the C57Bl6/J background. Virgin female or male mice were used for analysis at the age of 3-6 months depending on the length of treatment.

Fluoxetine hydrochloride USP (Flx, 20mg/kg/day) (Combi-Blocks, San Diego, California) was added aseptically to the drinking water and bottles were replaced every other day. Propranolol (Prop, 0.5mg/day) (Sigma, St. Louis, Missouri) was added aseptically to the drinking water. Recombinant lipocalin-2 (Lcn2, 200ng/g/day in PBS) prepared as previously described (38) or lorcaserin hydrochloride (Lorca, 3mg/Kg/day) in PBS (AbMole BioScience, Houston) was injected intra-peritoneally at 6:45 p.m. Vehicle controls were injected with a similar volume of PBS. Treatments represented in Figure 4B-F and Figure 6A-D were done simultaneously using the same vehicle-treated and Flx-treated groups.

Physiological measurements

For body weight measurements over 6 weeks, animals were housed in home cages by groups of 5 with water and chow *ad libitum*. Measurements were taken every week between 9-10 a.m.

For body weight and food intake over 4 or 5 days, animals were individualized in home cages with water and chow *ad libitum*. After 4 days of acclimation, basal body weight was measured daily, between 9-10 a.m., and food was weighted daily at 9 a.m. and 6:45 p.m., for 4 or 5 additional days. Mice were then treated with vehicle- or Flx-water or Flx/prop-water (or injected with Lcn2 or Lorca or vehicle). At the beginning of the treatment chow was replace with fresh chow (150-170 g) and body weight and food consumption were measured as above. Percentage of body weight was represented relative to the average of the last 3 measurements of body weight prior treatment.

For food intake measurements over 14h, animals were individualized in home cages with water and chow *ad libitum*. After 4 days of acclimation, mice were weighted to ensure that no difference in body weight existed between groups (Supplemental Figure 8, A and B). They were then treated with vehicle or Flx-water at 6:45 p.m., chow was replaced with fresh chow (150-170 g) and food was weighted at 9 a.m. the next morning.

Energy expenditure was assessed through measurement by indirect calorimetry of oxygen consumption (V_{O2}), carbon dioxide production (V_{CO2}), heat production and locomotor activity using an automated home cage phenotyping system (TSE-Systems), except for Supplementary Figure 2, L and O, for which a 6-chambers Oxymax system (Columbus Instruments, Ohio) was used. Mice were singled-housed in a climate-controlled chamber (temperature: 22°C; humidity: 55%; 12 h light-dark cycle) with water and chow *ad libitum*. After 48 h (Oxymax) or 7 days (TSE) of adaptation to social isolation, mice were treated with vehicle or Flx for 5 days (for Figure 1C, mice were treated with vehicle or Flx for a period of 6 weeks, including adaptation to social isolation and recording time). Data were collected and analyzed as recommended by the manufacturers. Day-by-day values or averaged measurements of the last 4 days are represented as indicated. Locomotor activity was recorded as beam breaks converted into distance/velocity, measuring activity in 3-D. Beam breaks were analyzed by custom software from the metabolic cage. Respiratory exchange ratio (RER) and energy expenditure were calculated from oxygen consumption and carbon dioxide production data. In the TSE system day 1-3 and day 4-6 measurements were used for energy expenditure assessment.

Fat content and body temperature were measured using magnetic resonance imaging (EchoMRI, Houston, TX). Gonadal and subcutaneous white adipose tissue was dissected and weighted at the time of euthanasia and represented relative to body weight.

iDISCO+ Whole-Brain Clearing, Labeling, Imaging and ClearMap Analysis

Female mice were individualized in home cages with water and chow *ad libitum*. After 4 days of acclimation, they were fasted overnight. In the morning (9:00 a.m.) food was added and water was replaced with vehicle- or Flx-water. Mice were euthanized after 2h and transcardially perfused with PBS followed by 4% paraformaldehyde (PFA). Brains were post-fixed for 24 h, after which immunolabeling with rabbit c-Fos

1:4000 (Synaptic Systems Cat# 226 003, RRID:AB_2231974) and whole-brain clearing were performed according to previously established protocols (46). For acquisition, cleared samples were imaged in a sagittal orientation (left lateral side up) on a light-sheet microscope (LaVision Biotec) equipped with a sCMOS camera and LVMI-Fluor 4x objective lens equipped with a 6 mm working distance dipping cap. Version v144 and v210 of Inspector Microscope controller software was used. Samples were scanned in the 640 nm channel. Images were taken every 6 µm and reconstructed with the ClearMap software for quantification or Imaris 9.1 software for visualization. For autofluorescence, the 480 nm channel was used with a 1.3x objective lens. Whole-brain were analyzed using the ClearMap software (latest version available from https://www.idisco.info/) (see also (46, 47)).

Immunohistofluorescence

Mice were individualized in home cages with water and chow *ad libitum*. For the 2h treatment, after 4 days of acclimation, mice were fasted overnight. In the morning (9:00 a.m.) food was added and water was replaced with vehicle- or Flx-water, and mice were euthanized after 2h. For 14h treatment, after 4 days of acclimation, mice were treated with vehicle- or Flx-water at 6:45 p.m., and chow was replaced with fresh chow (150-170 g). Flx-treated mice were randomized in three groups: one group was euthanized immediately, a second group was euthanized 24h after Flx was withdrawn and replaced with vehicle (14h Flx + 1 day withdrawal), the third group was euthanized 48h after Flx was withdrawn and replaced with vehicle (14h Flx + 2 days withdrawal). Vehicle mice were also randomized in 3 sub-groups that were respectively euthanized with the Flx, 1- or 2-days withdrawal groups. Since no difference was found between the 3 vehicle sub-groups, their data were pooled for analysis. Mice were euthanized between 9 and 11 a.m. For the withdrawal experiment following a long-term treatment, mice were treated with vehicle or Flx for 5 weeks. Then, Flx-treated mice were randomized in two groups: one group was kept in Flx for one more week and euthanized at week 6 from day 0 of treatment, a second group was kept with no treatment for 2 more weeks and euthanized at week 7 from day 0 of treatment (5 weeks Flx + 2 weeks withdrawal), the third group was kept with no treatment for 4 weeks and euthanized at week 9 from day 0 of treatment (5

weeks Flx + 4 weeks withdrawal). Vehicle mice were also randomized in 3 sub-groups that were respectively euthanized with the Flx-treated group or with the 2 weeks withdrawal group or with the 4 weeks withdrawal group. Since no difference was found between the 3 control sub-groups, their data were pooled for analysis. Mice were euthanized between 9 and 11 a.m.

Euthanized mice were transcardially perfused with PBS followed by 4% PFA. Brains were then post-fixed for 12-24 h and sectioned to a thickness of 50 µm using a floating vibratome. Primary antibodies used for immunohistochemistry were: rabbit c-Fos 1:1000 (Cell Signaling Technology 2250, RRID:AB_2247211), guinea pig c-Fos 1:1000 (Synaptic Systems 226 004, RRID:AB_2619946), rabbit Tph2 1:1000 (Novus NB100-74555, RRID:AB_1049988), rabbit POMC 1:4000 (Phoenix Pharmaceuticals H-029-30, RRID:AB_2307442), sheep α-MSH 1:10000 (Millipore AB5087, RRID:AB_91683), rabbit NPY 1:1000 (Abcam ab221145), mouse Htr2c 1:200 (Santa Cruz sc-17797). Secondary antibodies were Alexa Fluor conjugated (Alexa 488-donkey anti-sheep, Invitrogen A11015; Alexa 488-donkey anti-rabbit, Jackson ImmunoResearch 711-545-152; Alexa 488-goat anti-guinea, Invitrogen A11073; Alexa 594-donkey anti-rabbit, Jackson ImmunoResearch 711-585-152). Antibodies were previously validated. All images were captured using confocal microscopy (Zeiss, Germany). For number of cells, graphs represent the sum of cells counted in 3 slides/mouse and averaged per group. Integrated density values were calculated using the Fiji software (48) and the average of 3 slides/mouse was represented.

Cell culture, in vitro treatments

SH-SY5Y cells (ATCC) were cultured in DMEM:F12 10% FBS and differentiated for 5 days with B-27 Plus Supplement (Gibco A3582801), GlutaMAX (Gibco 35050061) and all-trans-retinoic acid (ATRA, Abcam ab141962) in Neurobasal Plus Medium (Gibco A3582901) prior to SSRI treatment. Fluoxetine (Combi-Blocks, San Diego, California), paroxetine, fluvoxamine, sertraline and escitalopram (Sigma Aldrich, St. Louis, Missouri) we dissolved at 10 mM in NaCl 0.9% and added to the medium to the final concentration of 3 µM. Cells were treated for 2h for Western blotting or 4h for gene expression.

Western blotting

Proteins were extracted from cells using the PhosphoSafe™ Extraction Reagent (Millipore, Burlington, MA) and 8-10 μg of extract were analyzed by Western blot using the following antibodies: phospho-STAT3-Tyr705 (Cell Signaling, Danvers, Massachusetts, 9131), phosphor-STAT3-Ser727 (1:1000 Cell Signaling, 9134S), STAT3 (1:1000, Cell Signaling, 9139), GAPDH (1:5000, Cell Signaling, 5174), phospho-CREB (1:1000, 9198), CREB (1:1000, Cell Signaling, 9104) followed by incubation with HPR-conjugated anti-rabbit (1:2000, Abcam NA934V) or anti-mouse (1:2000, GE Healthcare UK NXA931) IgG antibodies and detection with ECL-Western blot reagent (Advansta, San Jose, California). Imaged blots were quantified using the Fiji software (48). For all antibodies, validation is available on the manufacturer's website.

Gene expression

RNA was purified from dissected hypothalami using TRIzol (Invitrogen, Grand Island, New York). Real-time PCR (qPCR) was performed using the Taq SYBR Green Power PCR Master Mix (Invitrogen) on a CFX Connect instrument (Bio-Rad, Hercules, California); *Hprt* amplification was used as an internal reference for each sample. Verification of amplicon specificity was tested through a BLAST search and dissociation curves analysis was performed in every experiment. Primers sequences are indicated in Supplemental Table 1.

Marble burying test

Twelve glass marbles were evenly spaced in three rows, on approx. 5 cm layer of sawdust bedding lightly pressed down to make a flat even surface, in a plastic cage. The day before euthanasia each mouse was placed in the cage and left for 30min after which the number of marbles buried with sawdust was counted (49).

Statistical analysis

All values are expressed as mean ± SEM. Group sizes were determined by performing a power calculation to lead to an 80% chance of detecting a significant difference ($p \leq 0.05$). All values use biological replicates and are indicated by group size (n) in figure legends and/or by graphs plotted with individual values. Statistical analyses were performed using one-way ANOVA or two-way ANOVA followed by Sirak's or Tukey's test or ANCOVA, to compare means of three or more groups, and unpaired two-tailed Student's t-test to compare means of two groups, as indicated in figure legends. In all figures * $p \leq 0.05$, ** $p \leq 0.01$, *** $p \leq 0.001$, **** $p \leq 0.0001$. All statistical analyses were performed using GraphPad Prism (GraphPad Software), except for the energy expenditure experiments for which CalR (50) was used.

Study approval

The Columbia University Institutional Animal Care and Use Committee (IACUC) approved all procedures.

Author contributions

Conceptualization; M.J.O., P.D. Methodology: M.J.O., M.S., P.D. Investigation: M.J.O, M.S., A.I., K.P., F.M. Data analysis: M.J.O., M.S., P.D. Funding acquisition: P.D. Expertise and feedback: J.M.F., P.C. Writing: M.J.O., P.D.

Acknowledgments

We thank Drs. P, Cohen, G. Karsenty, S. Kousteni, A. Nectow and L. Zeltser for sharing reagents/equipment, providing advice and for commenting on the manuscript. Images were collected in The Rockefeller University Bio-Imaging Resource Center.

Funding

National Institutes of Health grant (NIA) AG032959 (P.D.). JPB Foundation (J.M.F.). Robertson Therapeutic Development Fund (M.S. and J.M.F.). National Institutes of Health grant DK120869 (M.S). Kavli NSI Postdoctoral Fellowship (M.S.)

Competing interests

The authors declare no competing interests.

Data and materials availability

This study did not generate new unique reagents.

REFERENCES

1. Kane SP. https://clincalccom/DrugStats/Drugs/FluoxetineHydrochloride. ClinCalc DrugStats Database, Version 21.1; 2020.
2. Wong DT, et al. Prozac (fluoxetine, lilly 110140), the first selective serotonin uptake inhibitor and an antidepressant drug: Twenty years since its first publication. *Life Sciences.* 1995;57(5):411-41.
3. Fox M, et al. A pharmacological analysis of mice with a targeted disruption of the serotonin transporter. *Psychopharmacology.* 2007;195(2):147-66.
4. Heisler LK, et al. Serotonin reciprocally regulates melanocortin neurons to modulate food intake. *Neuron.* 2006;51(2):239-49.
5. Xu Y, et al. 5-HT2CRs expressed by pro-opiomelanocortin neurons regulate energy homeostasis. *Neuron.* 2008;60(4):582-9.
6. Heisler LK, et al. Fluoxetine decreases fat and protein intakes but not carbohydrate intake in male rats. *Pharmacol Biochem Behav.* 1997;58(3):767-73.
7. Heisler LK, et al. Reduction of fat and protein intakes but not carbohydrate intake following acute and chronic fluoxetine in female rats. *Pharmacol Biochem Behav.* 1999;63(3):377-85.
8. Voigt JP, and Fink H. Serotonin controlling feeding and satiety. *Behav Brain Res.* 2015;277(14-31.
9. Burke LK, and Heisler LK. 5-hydroxytryptamine medications for the treatment of obesity. *J Neuroendocrinol.* 2015;27(6):389-98.
10. Jensen-Otsu E, and Austin GL. Antidepressant Use is Associated with Increased Energy Intake and Similar Levels of Physical Activity. *Nutrients.* 2015;7(11):9662-71.
11. Kivimäki M, et al. Antidepressant Medication Use, Weight Gain, and Risk of Type 2 Diabetes. *Diabetes care.* 2010;33(12):2611.
12. Lee SH, et al. Is increased antidepressant exposure a contributory factor to the obesity pandemic? *Translational psychiatry.* 2016;6(3):e759.
13. Carvalho AF, et al. The Safety, Tolerability and Risks Associated with the Use of Newer Generation Antidepressant Drugs: A Critical Review of the Literature. *Psychotherapy and psychosomatics.* 2016;85(5):270-88.
14. Gafoor R, et al. Antidepressant utilisation and incidence of weight gain during 10 years' follow-up: population based cohort study. *BMJ (Clinical research ed).* 2018;361(k1951.
15. Andersohn F, et al. Long-term use of antidepressants for depressive disorders and the risk of diabetes mellitus. *Am J Psychiatry.* 2009;166(5):591-8.

16. Cascade E, et al. Real-World Data on SSRI Antidepressant Side Effects. *Psychiatry (Edgmont (Pa : Township)).* 2009;6(2):16-8.
17. Lockhart P, and Guthrie B. Trends in primary care antidepressant prescribing 1995-2007: a longitudinal population database analysis. *The British journal of general practice : the journal of the Royal College of General Practitioners.* 2011;61(590):e565-72.
18. Bolo NR, et al. Brain pharmacokinetics and tissue distribution in vivo of fluvoxamine and fluoxetine by fluorine magnetic resonance spectroscopy. *Neuropsychopharmacology.* 2000;23(4):428-38.
19. Yadav VK, et al. A serotonin-dependent mechanism explains the leptin regulation of bone mass, appetite, and energy expenditure. *Cell.* 2009;138(5):976-89.
20. Aponte Y, et al. AGRP neurons are sufficient to orchestrate feeding behavior rapidly and without training. *Nature neuroscience.* 2011;14(3):351-5.
21. Varela L, and Horvath TL. Leptin and insulin pathways in POMC and AgRP neurons that modulate energy balance and glucose homeostasis. *EMBO reports.* 2012;13(12):1079-86.
22. Balthasar N, et al. Divergence of melanocortin pathways in the control of food intake and energy expenditure. *Cell.* 2005;123(3):493-505.
23. Dahlin A, et al. Expression profiling of the solute carrier gene family in the mouse brain. *J Pharmacol Exp Ther.* 2009;329(2):558-70.
24. Bengel D, et al. Altered brain serotonin homeostasis and locomotor insensitivity to 3, 4-methylenedioxymethamphetamine ("Ecstasy") in serotonin transporter-deficient mice. *Mol Pharmacol.* 1998;53(4):649-55.
25. Ren J, et al. Anatomically Defined and Functionally Distinct Dorsal Raphe Serotonin Sub-systems. *Cell.* 2018;175(2):472-87.e20.
26. Nectow AR, et al. Identification of a Brainstem Circuit Controlling Feeding. *Cell.* 2017;170(3):429-42.e11.
27. Samuels BA, et al. Serotonin 1A and Serotonin 4 Receptors: Essential Mediators of the Neurogenic and Behavioral Actions of Antidepressants. *The Neuroscientist : a review journal bringing neurobiology, neurology and psychiatry.* 2016;22(1):26-45.
28. Hjorth S, et al. Serotonin autoreceptor function and antidepressant drug action. *Journal of psychopharmacology (Oxford, England).* 2000;14(2):177-85.
29. Hannon J, and Hoyer D. Molecular biology of 5-HT receptors. *Behav Brain Res.* 2008;195(1):198-213.
30. Sprouse JS, and Aghajanian GK. (-)-Propranolol blocks the inhibition of serotonergic dorsal raphe cell firing by 5-HT1A selective agonists. *Eur J Pharmacol.* 1986;128(3):295-8.
31. Gautron L, et al. Neural control of energy balance: translating circuits to therapies. *Cell.* 2015;161(1):133-45.
32. Ortuno MJ, et al. Serotonin-reuptake inhibitors act centrally to cause bone loss in mice by counteracting a local anti-resorptive effect. *Nature medicine.* 2016;22(10):1170-9.
33. Oury F, et al. CREB mediates brain serotonin regulation of bone mass through its expression in ventromedial hypothalamic neurons. *Genes & development.* 2010;24(20):2330-42.
34. Berglund ED, et al. Serotonin 2C receptors in pro-opiomelanocortin neurons regulate energy and glucose homeostasis. *The Journal of clinical investigation.* 2013;123(12):5061-70.
35. Yeo GS, and Heisler LK. Unraveling the brain regulation of appetite: lessons from genetics. *Nature neuroscience.* 2012;15(10):1343-9.
36. Quarta C, et al. POMC neuronal heterogeneity in energy balance and beyond: an integrated view. *Nature metabolism.* 2021;3(3):299-308.

37. Bates S, et al. STAT3 signalling is required for leptin regulation of energy balance but not reproduction. *Nature.* 2003;421(856-9.
38. Mosialou I, et al. MC4R-dependent suppression of appetite by bone-derived lipocalin 2. *Nature.* 2017;543(7645):385-90.
39. Dulawa SC, et al. Effects of chronic fluoxetine in animal models of anxiety and depression. *Neuropsychopharmacology.* 2004;29(7):1321-30.
40. O'Leary OF, et al. Chronic fluoxetine treatment increases expression of synaptic proteins in the hippocampus of the ovariectomized rat: role of BDNF signalling. *Psychoneuroendocrinology.* 2009;34(3):367-81.
41. Felsing DE, et al. Ligand-directed serotonin 5-HT(2C) receptor desensitization and sensitization. *Eur J Pharmacol.* 2019;848(131-9.
42. Petropoulou PI, et al. Lipocalin-2 is an anorexigenic signal in primates. *eLife.* 2020;9(
43. Greenfield JR, et al. Modulation of blood pressure by central melanocortinergic pathways. *N Engl J Med.* 2009;360(1):44-52.
44. Haws R, et al. Effect of setmelanotide, a melanocortin-4 receptor agonist, on obesity in Bardet-Biedl syndrome. *Diabetes Obes Metab.* 2020;22(11):2133-40.
45. Clément K, et al. Efficacy and safety of setmelanotide, an MC4R agonist, in individuals with severe obesity due to LEPR or POMC deficiency: single-arm, open-label, multicentre, phase 3 trials. *The lancet Diabetes & endocrinology.* 2020;8(12):960-70.
46. Renier N, et al. Mapping of Brain Activity by Automated Volume Analysis of Immediate Early Genes. *Cell.* 2016;165(7):1789-802.
47. Renier N, et al. iDISCO: a simple, rapid method to immunolabel large tissue samples for volume imaging. *Cell.* 2014;159(4):896-910.
48. Schindelin J, et al. Fiji: an open-source platform for biological-image analysis. *Nat Methods.* 2012;9(7):676-82.
49. Angoa-Perez M, et al. Marble burying and nestlet shredding as tests of repetitive, compulsive-like behaviors in mice. *J Vis Exp.* 201382):50978.
50. Mina AI, et al. CalR: A Web-Based Analysis Tool for Indirect Calorimetry Experiments. *Cell metabolism.* 2018;28(4):656-66.e1.

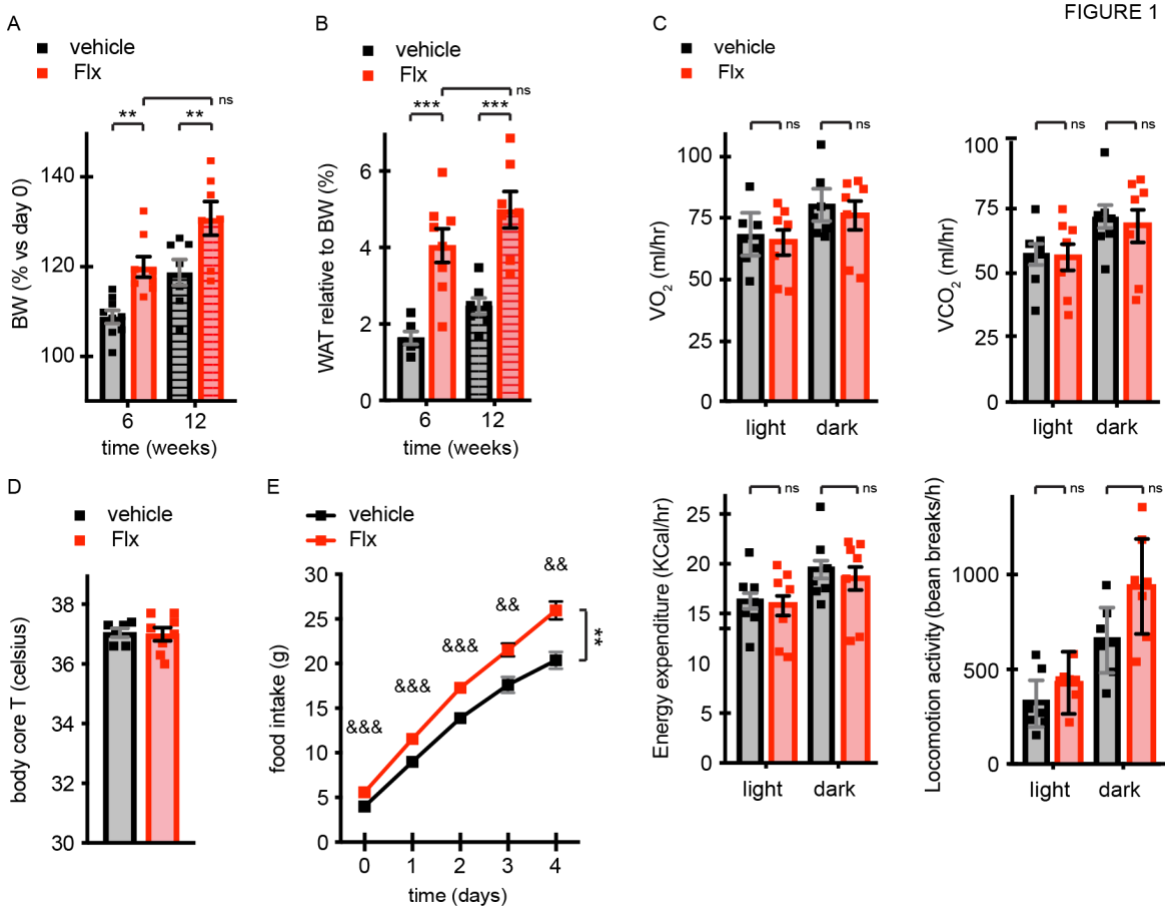

Figure 1. Long-term oral treatment with fluoxetine increases body weight and adiposity by specifically enhancing food intake.

(**A**) Percentage of body weight (BW) relative to day 0 in WT females treated with vehicle or Flx for 6 weeks (plain bars, n=8-9 mice/group, representative of 6 independent experiments) and 12 weeks (hatched bars, n=7 mice/group).

(**B**) Percentage of white adipose tissue (WAT) content relative to BW at the end of the 6-weeks (n=6-8 mice/group) and 12-weeks (n=7 mice/group) treatment period.

(**C-E**) WT females treated with vehicle or Flx for 6 weeks. (**C**) Energy expenditure measured by oxygen consumption (V_{O2}), carbon dioxide production (V_{CO2}), heat production and locomotor activity recorded over the last 3 days of treatment (n=7 mice/group). (**D**) Core body temperature (T) at the end of the treatment period (n=6-8 mice/group). (**E**) Cumulative food intake measured over the last 5 days of treatment (n=6-7 mice/group, representative of two independent experiments).

Values are mean ± SEM. *P≤0.05; **P≤0.01; ***P≤0.001; ns, not significant; by two-way analysis of variance (ANOVA) followed by Sidak's test (**A, B**, Locomotion activity in **C**), analysis of covariance (ANCOVA) (**C**, except for Locomotion activity) and paired Student's test (**E**) compared to vehicle. $^{\&\&}P \leq 0.01$, $^{\&\&\&}P \leq 0.001$ Student's test of Flx compared to vehicle, analyzed for each time point.

FIGURE 2

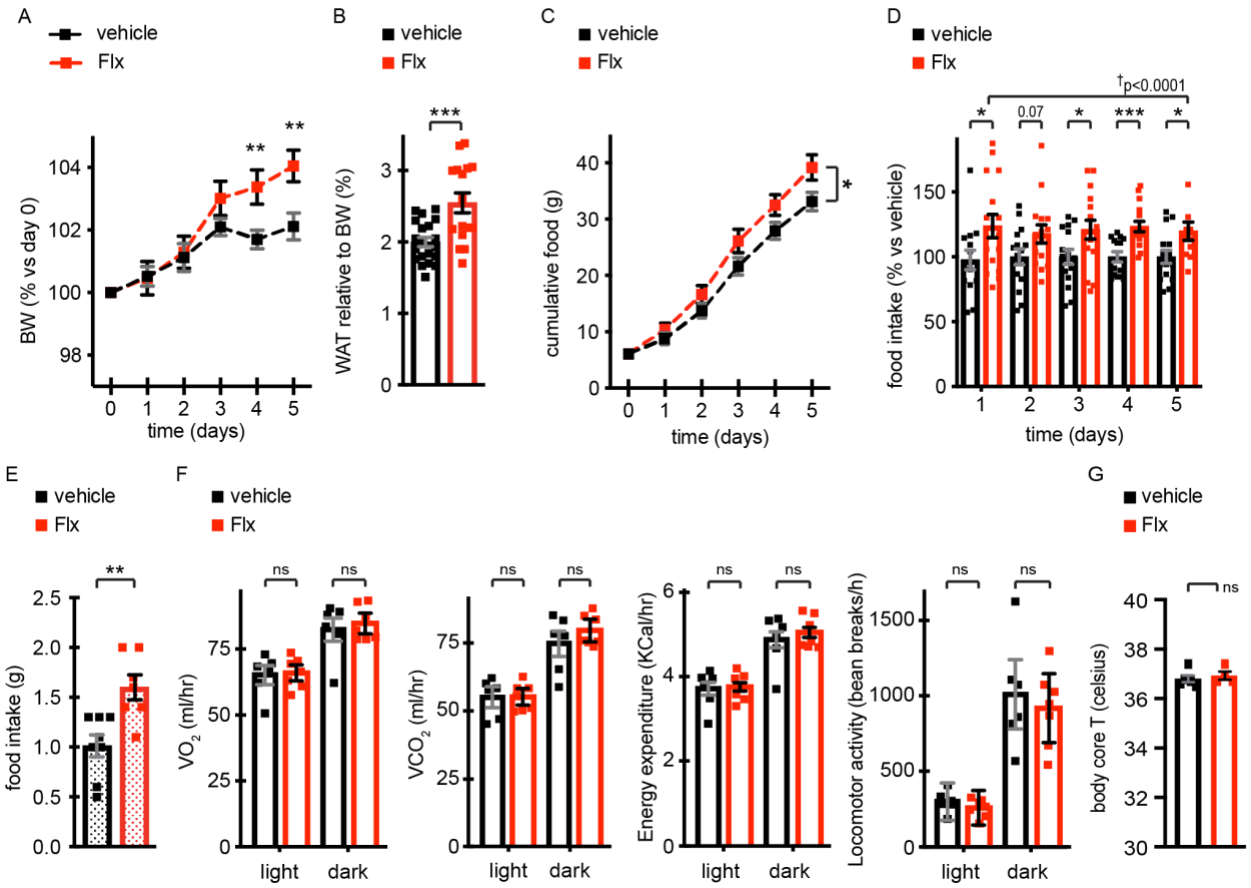

Figure 2. A short-term treatment with fluoxetine induces a rapid increase of feeding.

(**A-C**) WT females treated with vehicle or Flx for 5 days. (**A**) Percentage of BW relative to day 0 of treatment (n=16-17 mice/group). (**B**) Percentage of white adipose tissue (WAT) content relative to BW at the end of the treatment period (n=16-20 mice/group). (**C**) Daily percentage of food intake relative to vehicle (n=14-16 mice/group).

(**D**) Food intake of WT females treated with vehicle or Flx for 14h during the active (dark) phase of the day (n=7-8 mice/group).

(**E, F**) WT females treated with vehicle or Flx for 5 days. Energy expenditure measured by oxygen consumption (V_{O2}), carbon dioxide production (V_{CO2}), heat production and locomotor activity averaged over the last 4 days of treatment (**E**) (n=6-7 females/group). (**F**) Core body temperature at the end of the treatment period (n=4-6 mice/group).

Values are mean ± SEM. *P≤0.05; **P≤0.01; ***P≤0.001, ****P≤0.0001; ns, not significant; by unpaired Student's test compared to vehicle (**A-D**), analysis of covariance (ANCOVA) (**E**, except for Locomotion activity) or two-way analysis of variance (ANOVA) followed by Sidak's test (Locomotion activity at **E**), † paired Student's test of Flx compared to vehicle.

FIGURE 3

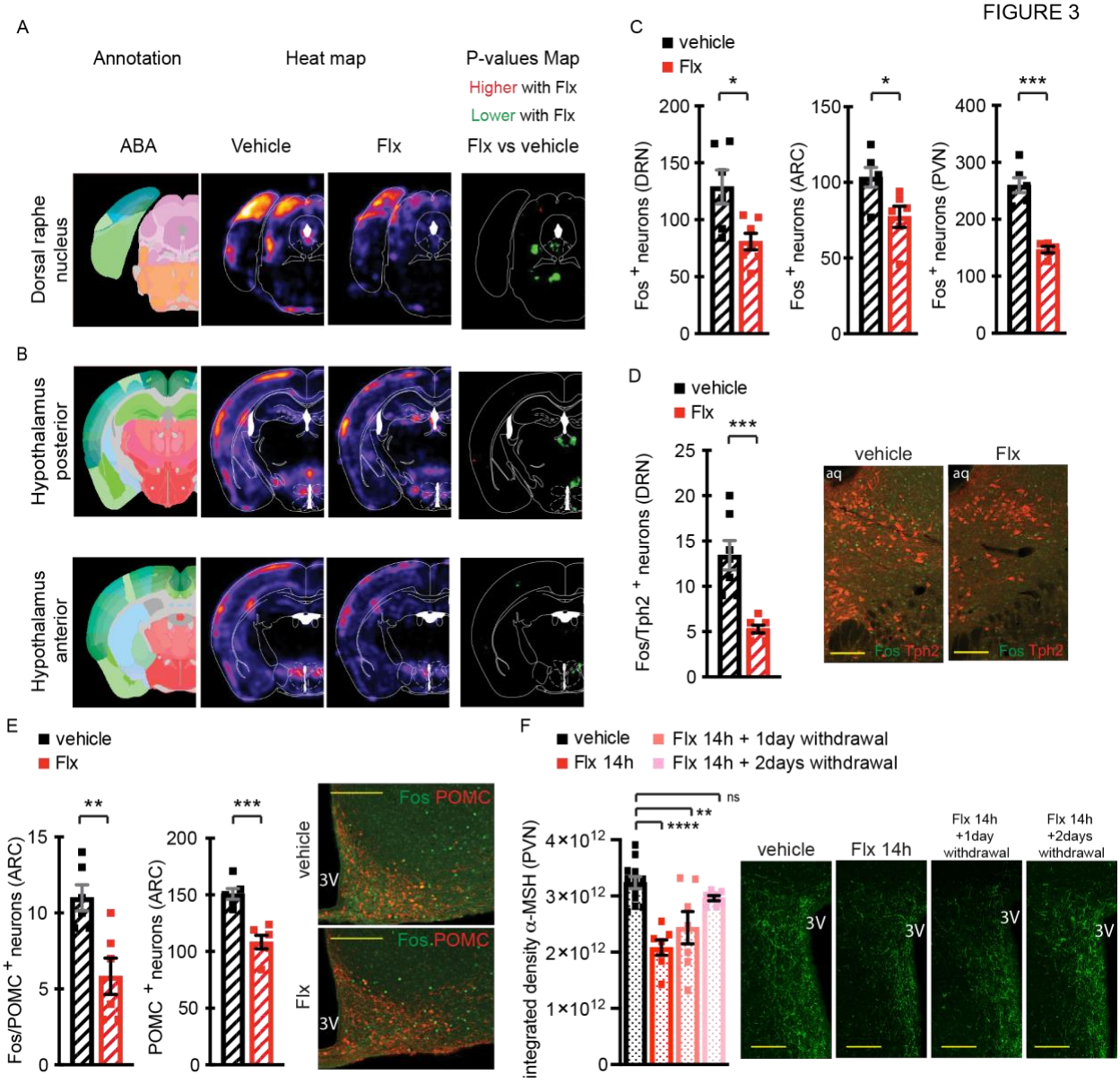

Figure 3. An acute treatment with fluoxetine decreases neurons^{DRN} activity and levels of hypothalamic α-MSH.

(**A, B**) iDISCO^{+} whole brain imaging and ClearMap analysis of c-Fos from compressed coronal views of the dorsal raphe nucleus (**A**) and hypothalamus (**B**) of WT female mice treated with vehicle or Flx for 2h (n=5-6 mice/group). Allen Brain Atlas (ABA). 4th column: Voxel-based statistical analysis. Regions with significantly different number of Fos^{+} cells in Flx- versus vehicle-conditions are highlighted.

(**C**) IHF validation of the iDISCO^{+} in brain slices of WT female mice treated with vehicle or Flx for 2h. Quantification of Fos^{+} neurons in dorsal raphe nucleus (DRN), arcuate nucleus (ARC), and paraventricular nucleus (PVN) (n=5-7 mice/group).

(**D, E**) Representative images and quantification following double immunohistofluorescence (IHF) as indicated, in brain slices of WT female mice treated with Flx or vehicle for 2h (**D**, n=7 mice/group; **E**, n=6 mice/group).

(**F**) Representative IHF images and levels of α-MSH in PVN neurons quantified as integrated density in brain slices of WT female mice treated with vehicle or Flx for 14h. Fluoxetine was then withdrawn in some of the groups as indicated (n=12 vehicle, 7 mice/other groups).

aq, aqueduct; 3V, third ventricle. Scale bar, 200µm. Values are mean ± SEM. *P≤0.05; **P≤0.01; ***P≤0.001, ****P≤0.0001; ns, not significant; by unpaired Student's test compared to vehicle (**C-E**) or by one-way analysis of variance (ANOVA) followed by Dunnett's test (**F**).

FIGURE 4

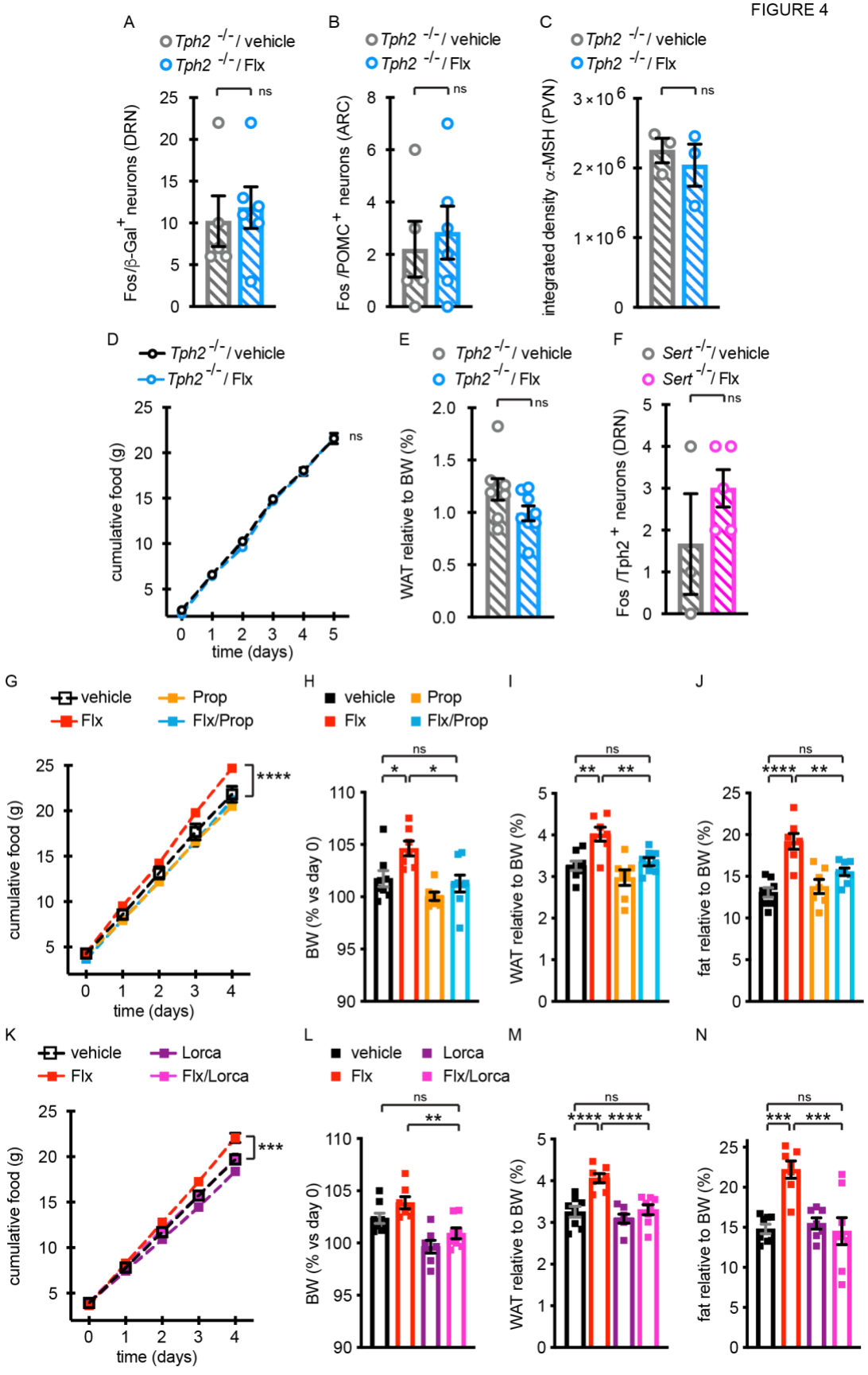
A
Tph2 -/- / vehicle
Tph2 -/- / Flx
Fos/β-Gal+ neurons (DRN)
ns
B
Tph2 -/- / vehicle
Tph2 -/- / Flx
Fos /POMC+ neurons (ARC)
ns
C
Tph2 -/- / vehicle
Tph2 -/- / Flx
integrated density α-MSH (PVN)
ns
D
Tph2 -/- / vehicle
Tph2 -/- / Flx
cumulative food (g)
time (days)
ns
E
Tph2 -/- / vehicle
Tph2 -/- / Flx
WAT relative to BW (%)
ns
F
Sert -/- / vehicle
Sert -/- / Flx
Fos /Tph2+ neurons (DRN)
ns
G
vehicle
Flx
Prop
Flx/Prop
cumulative food (g)
time (days)
****
H
vehicle
Flx
Prop
Flx/Prop
BW (% vs day 0)
ns
* *
I
WAT relative to BW (%)
ns
** **
J
fat relative to BW (%)
ns
**** **
K
vehicle
Flx
Lorca
Flx/Lorca
cumulative food (g)
time (days)
***
L
vehicle
Flx
Lorca
Flx/Lorca
BW (% vs day 0)
ns
**
M
WAT relative to BW (%)
ns
**** ****
N
fat relative to BW (%)
ns
*** ***

Figure 4. The short-term fluoxetine-induced hyperphagia is serotonin-dependent and can be countered by pharmacologically inhibiting Htr1a or activating Htr2c signaling.

(**A, B**) Immunohistofluorescence (IHF) in brain slices of *Tph2*$^{-/-}$ female mice treated with Flx or vehicle for 2h. (**A**) Quantification of Fos/ßGal^{+} neurons in DRN or (**B**) Fos/POMC^{+} neurons in ARC (n=5-6 mice/group). (**C**) IHF in brain slices of *Tph2*$^{-/-}$ females treated with Flx or vehicle for 14h. Graph represents levels of α-MSH measured as integrated density (n=3 mice/group).

(**D, E**) *Tph2*$^{-/-}$ females treated with Flx or vehicle for 5 days (n=8 mice/group). (**D**) Cumulative food. (**E**) Percentage of white adipose tissue (WAT) content relative to BW.

(**F**) Quantification of Fos/Tph2^{+} neurons in DRN by IHF in brain slices of *Sert*$^{-/-}$ female mice treated with Flx or vehicle for 2h (n=3-5 mice/group).

(**G-J**) WT females treated for 4 days with vehicle, Flx, propranolol (Prop) or both drugs (n=7-8 mice/group). (**G**) Cumulative food intake. (**H**) Percentage of BW relative to day 0 of treatment. (**I**) Percentage of WAT content relative to BW. (**J**) Fat content measured by EchoMRI^{TM} relative to BW.

(**K-N**) WT females treated for 4 days with vehicle, Flx, lorcaserin (Lorca) or both drugs (n=7-8 mice/group). (**K**) Cumulative food intake. (**L**) Percentage of BW relative to day 0 of treatment. (**M**) Percentage of WAT content relative to BW. (**N**) Fat content measured by EchoMRI^{TM} relative to BW.

Values are mean ± SEM. *P≤0.05; **P≤0.01; ***P≤0.001; ****P≤0.0001; ns, not significant; by unpaired (**A-C, E, F**) or paired (**D**) Student's test compared to vehicle, by two-way analysis of variance (ANOVA) (**G, K**) or one-way ANOVA (**H-J, L-N**) followed by Tukey's test.

FIGURE 5

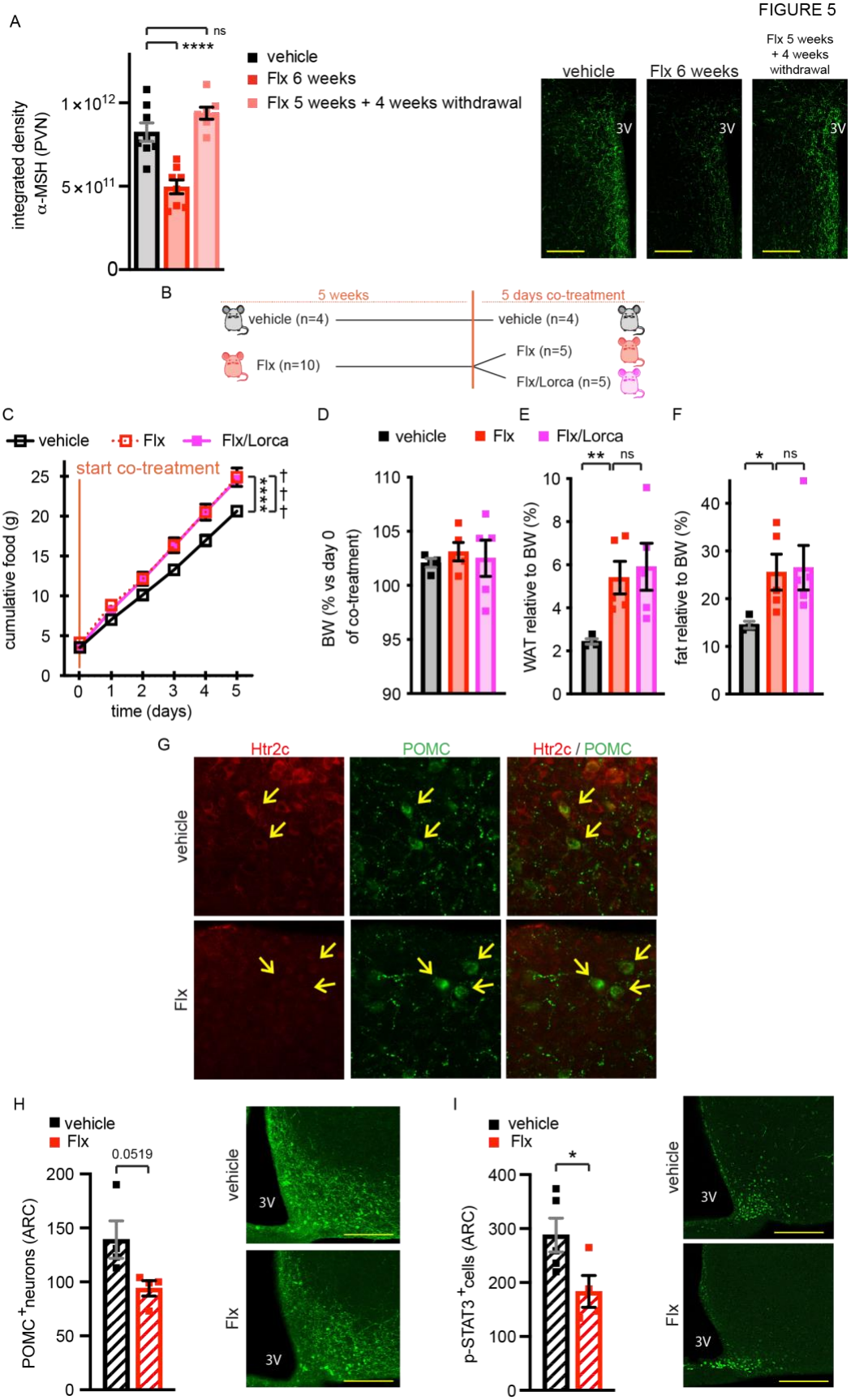
A
ns
****
vehicle
Flx 6 weeks
Flx 5 weeks + 4 weeks withdrawal
integrated density α-MSH (PVN)
1×10^12
5×10^11
0
vehicle
Flx 6 weeks
Flx 5 weeks + 4 weeks withdrawal
3V
B
5 weeks
5 days co-treatment
vehicle (n=4)
vehicle (n=4)
Flx (n=10)
Flx (n=5)
Flx/Lorca (n=5)
C
vehicle
Flx
Flx/Lorca
start co-treatment
cumulative food (g)
time (days)
D
BW (% vs day 0 of co-treatment)
E
WAT relative to BW (%)
F
fat relative to BW (%)
G
Htr2c
POMC
Htr2c / POMC
vehicle
Flx
H
vehicle
Flx
0.0519
POMC+neurons (ARC)
I
p-STAT3+cells (ARC)

Figure 5. A long-term treatment with fluoxetine impairs Htr2c signaling, Stat3 phosphorylation and α-MSH production in hypothalamic neurons.

(**A**) Representative images of immunohistofluorescence (IHF) and levels of α-MSH quantified as integrated density in brain slices of WT female mice treated with Flx or vehicle for 6 weeks; Fluoxetine was then withdrawn in some of the groups as indicated (n=7-8 mice/group).

(**B-F**) WT female mice treated for 5 weeks with vehicle or Flx then treated with vehicle or Flx alone or Flx and lorcaserin (Lorca) for 5 more days (n=4-5 mice/group). (**B**) Experimental design. (**C**) Cumulative food intake. (**D**) Percentage of BW relative to day 0 of co-treatment. (**E**) Percentage of white adipose tissue (WAT) content relative to BW. (**F**) Fat content measured by EchoMRI^{TM} relative to BW.

(**G-I**) WT females treated with vehicle or Flx for 6 weeks (n=4 mice/group). (**G**) IHF representative images of Htr2c expression in POMC^{ARC} neurons. Arrows point out to POMC^{+} cells. Representative images and quantification of (**H**) POMC^{+} and (**I**) p-STAT3^{+} neurons in arcuate nuclei.

3V, third ventricle. Scale bar, 200µm. Values are mean ± SEM. Vehicle compared to Flx *P≤0.05; **P≤0.01; ****P≤0.0001. Vehicle compared to Flx/Lorca †††P≤0.001; ns, not significant; by one-way analysis of variance (ANOVA) (**A, E, F**), two-way ANOVA (**C**) followed by Tukey's test, or unpaired Student's test (**H, I**).

FIGURE 6

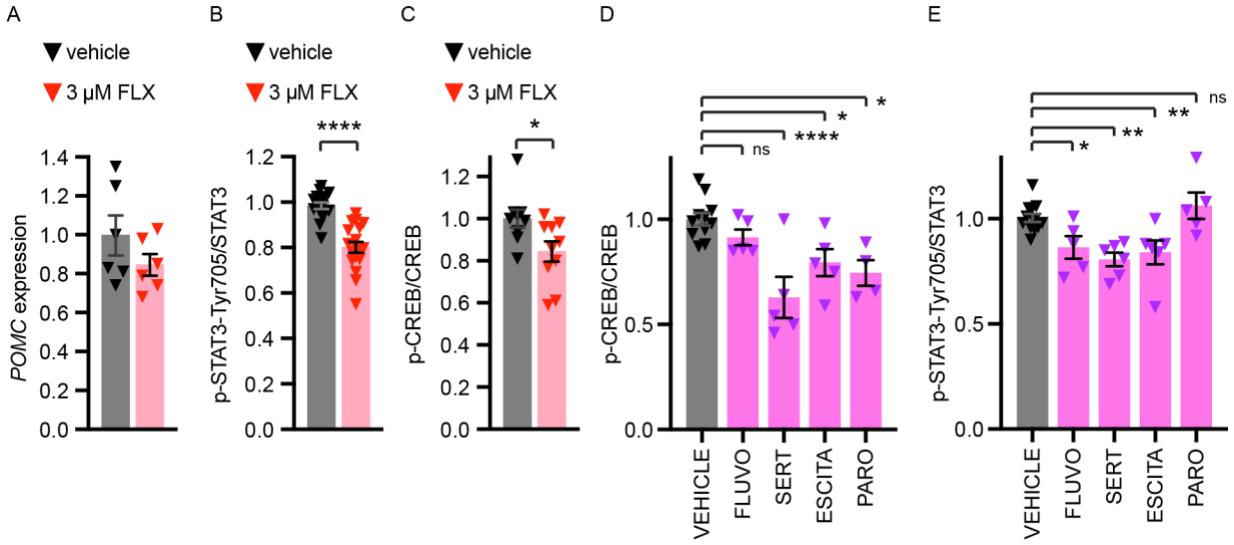

Figure 6. Fluoxetine and other SSRIs interfere with STAT3 and CREB phosphorylation in human neuronal cells.

SY5Y neuro-like cells differentiated for 5 days and treated with vehicle, Flx or other SSRIs as indicated. (**A**) Gene expression analysis of *POMC* by qPCR after 4h treatment. (**B, E**) Analysis of STAT3 or (**C, D**) CREB phosphorylation by Western blot after a 2h treatment with fluoxetine or vehicle.

FLUVO, fluvoxamine; SERT, sertraline; ESCITA, escitalopram; PARO, paroxetine. Values are mean ± SEM. *P≤0.05; **P≤0.01; ****P≤0.0001; ns, not significant; by Student's test compared to vehicle (**B,C**) or one-way analysis of variance (ANOVA) (**D, E**) followed by Dunnett's test.

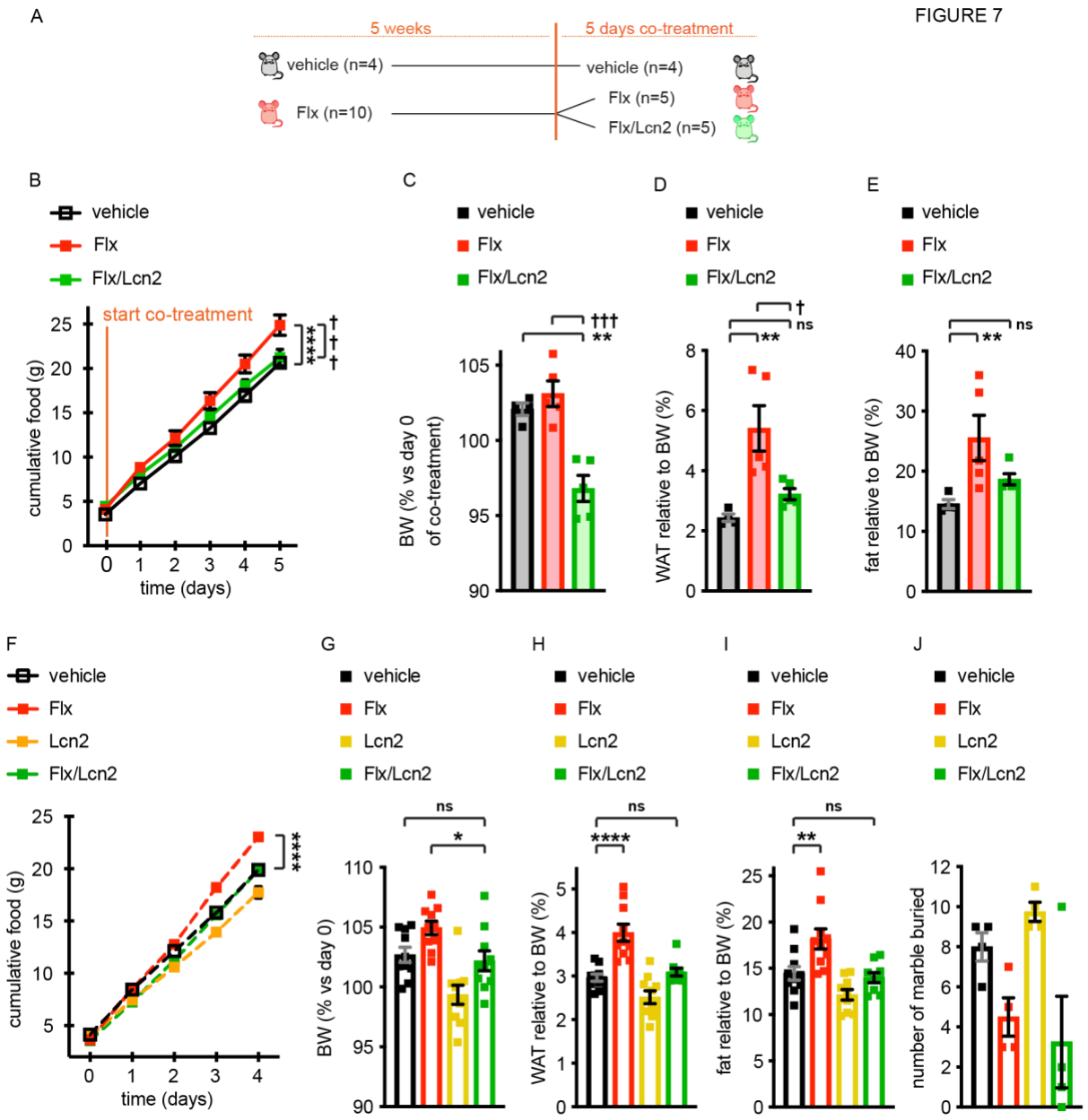

Figure 7. A co-treatment with lipocalin-2 can block the long-term effect of fluoxetine on feeding and body weight

(**A-E**) WT female mice treated for 5 weeks with vehicle or Flx then treated with vehicle, Flx or Flx and lipocalin-2 (Lcn2) for 5 more days (n=4-5 mice/group). (**A**) Experimental design. (**B**) Cumulative food intake. (**C**) Percentage of BW at last day of co-treatment relative to day 0 of co-treatment. (**D**) Percentage of white adipose tissue (WAT) content relative to BW. (**E**) Fat content relative to BW.

(**F-J**) WT female mice treated for 4 days with vehicle, Flx, Lcn2 or both drugs as indicated (n=10 mice/group). (**F**) Cumulative food intake. (**G**) Percentage of BW at last day of treatment relative to day 0. (**H**) Percentage of WAT content relative to BW. (**I**) Fat content relative to BW. (**J**) Marble-burying test.

Values are mean ± SEM. Vehicle compared to Flx *P≤0.05; **P≤0.01; ***P≤0.001; ****P≤0.0001. Flx compared to Flx/Lcn2 †P≤0.05; †††P≤0.001; ns, not significant; by two-way analysis of variance (ANOVA) (**B, F**) or one-way ANOVA (**C-E, G-J**) followed by Tukey's test.

FIGURE 8

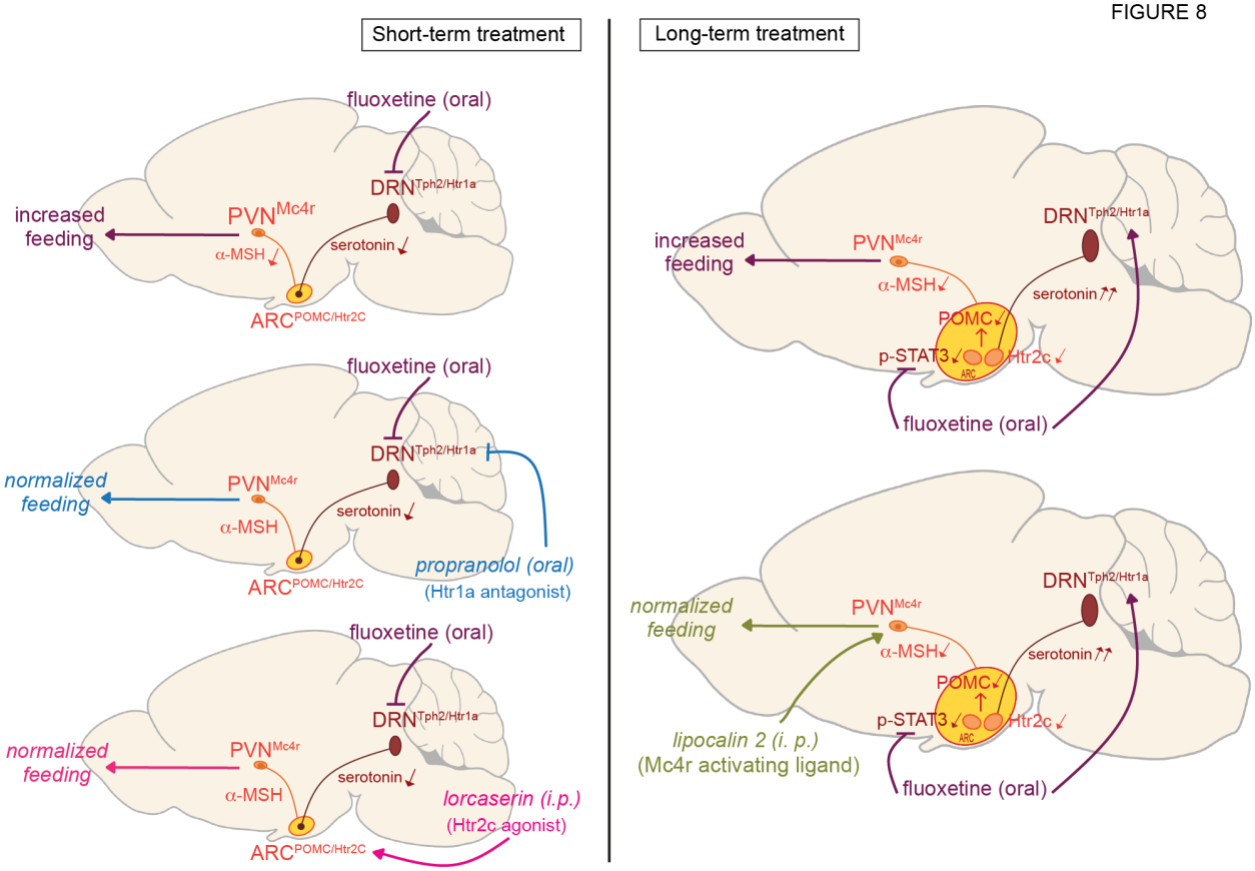

Figure 8. Mechanisms of Flx-induced short-term and long-term hyperphagia and weight gain.

In the short-term (left), within hours of oral treatment with Flx $DRN^{Tph2/Htr1a}$ neurons are inhibited, leading to a decrease in the serotonin-dependent activation of $ARC^{POMC/Htr2C}$-PVN^{Mc4r} neurons, which causes an increase in food intake (left, top). Blocking the Htr1a-dependent inhibition of $DRN^{Tph2/Htr1a}$ neurons using propranolol (left, middle) or activating $ARC^{POMP/Htr2C}$ neurons using lorcaserin (left, bottom) can therefore normalize feeding in this setting. Upon a long treatment **(right)**, however, Flx decreases Htr2c expression/signaling and inhibits Stat3 phosphorylation in ARC neurons resulting in reduced α-MSH production (right, top). This non-canonical and multifactorial activity of Flx explains the paradoxical hyperphagia and weight gain associated with its long-term use as well as the failure of lorcaserin to counter this effect. In contrast, a co-treatment with lipocalin-2, a Mc4r ligand, can normalize feeding and prevents weight gain (right, bottom).